Astron. Astrophys. 349, L49–L52 (1999)

ASTRONOMY AND ASTROPHYSICS

LETTER

Letter to the Editor

The X-ray diffuse emission from the Galactic Center

L. Sidoli[1,2] **and S. Mereghetti**[1]

[1] Istituto di Fisica Cosmica "G. Occhialini" – C.N.R., Via Bassini 15, I-20133 Milano, Italy (sidoli, sandro@ifctr.mi.cnr.it)
[2] Dipartimento di Fisica, Università di Milano, Sez. Astrofisica, Via Celoria 16, I-20133 Milano, Italy

Received 15 July 1999 / Accepted 9 August 1999

Abstract. A long BeppoSAX observation of the Galactic Center region shows that the spectrum of the diffuse X–ray emission from the SgrA Complex can be described with the sum of two thermal plasma models with temperatures of ∼0.6 keV and ∼8-9 keV. The spatial distribution of the diffuse emission is energy dependent. While the hard X–ray emission has a nearly symmetric distribution elongated along the Galactic Plane, the soft X–rays (E $<$ 5 keV) are remarkably well correlated with the triangular radio halo of SgrA East. The parameters derived for the soft component support the interpretation of the SgrA East shell in terms of an evolved supernova remnant.

Key words: ISM: supernova remnants – Galaxy: center – X-rays: general – X-rays: ISM

1. Introduction

The diffuse X–ray emission from the Galactic Center (GC) region was imaged for the first time with the Einstein Observatory in the 0.5–4 keV band (Watson et al. 1981) and later studied in more detail with several satellites (Kawai et al. 1988, Skinner et al. 1987, Koyama et al. 1989, 1996). The real nature of this emission is still an open issue. Though at least part of it can be due to the integrated emission from weak unresolved sources (Watson et al. 1981; Zane, Turolla & Treves 1996), there is evidence that a hot plasma, responsible for the observed emission lines, permeates the GC region. This was indicated by the Ginga discovery of a strong iron line at 6.7 keV with an equivalent width of $EW = 600 \pm 70$ eV (Koyama et al. 1989). More recently, the ASCA satellite confirmed the presence of a hot plasma (kT$\sim$ 10 keV) and discovered another diffuse component in the 6.4 keV Fe-line with an asymmetric spatial distribution with respect to the GC and well correlated with the distribution of the giant molecular clouds (Koyama et al. 1996). The data on the diffuse X–ray emission reported here were obtained during a survey of the GC performed with the BeppoSAX Narrow Field Instruments (Sidoli et al. 1998). The results on the point sources have been reported elsewhere (Sidoli et al. 1999a, 1999b).

Send offprint requests to: L. Sidoli

Sgr A Complex

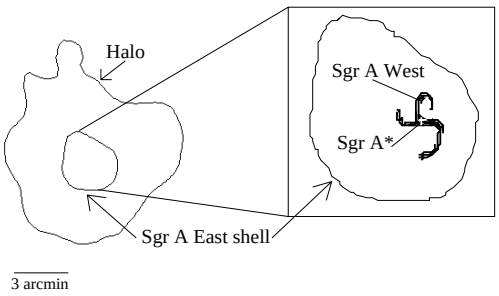

Fig. 1. A schematic view of the main radio structures in the SgrA Complex. North is to the top, East to the left. 1 arcmin corresponds to about 2.5 pc at 8.5 kpc.

2. The Galactic Center environment

Before presenting our results, we briefly describe the most important radio emitting sources present in the region within $\sim 8'$ from SgrA* covered by our observation (see Morris & Serabyn 1996 for a recent review). These extended sources are collectively known as the Sgr A Complex (Fig. 1).

The most peculiar object is the compact radio source SgrA* (Balick & Brown 1974). It has a radio luminosity of $\sim 2 \times 10^{34}$ ergs s^{-1} and a flux density rising as $S_\nu \propto \nu^{1/3}$ between a low frequency turnover at $\nu \sim$800 MHz and a cut–off at 2000–4000 GHz (Mezger, Duschl & Zylka 1996). Lo et al. (1998) measured an intrinsic size of less than 5.4×10^{13} cm with multi–wavelength VLBA observations. From the proper motion of the nearby IR stars a dark mass of 2.6×10^6 M$_\odot$ has been deduced to reside within a central volume of 10^{-6} pc^3 (Ghez et al. 1998). Sgr A* is generally considered to be a super–massive black hole due to its unique radio spectrum (see e.g. Krichbaum et al. 1998), its compactness, its location at the GC (Yusef-Zadeh, Choate & Cotton 1999) and its low proper motion ($\leq$40 km s^{-1}, Reid et al. 1999). The high energy emission of SgrA* is surprisingly low, corresponding to a 2–10 keV luminosity of only $\sim 10^{35}$ ergs s^{-1} (Koyama et al. 1996, Sidoli et al. 1999b), well below the Eddington limit for a 2 million solar masses black hole.

SgrA* is embedded in the ionized gas of SgrA West, an HII region with a characteristic "mini-spiral" shape of thermal radio emission. With an angular extent of $\sim 1'$, SgrA West is

the innermost and ionized part of the "Circumnuclear Disk", a structure of molecular gas extending from 1.7 pc up to about 7 pc from the GC and rotating around it (Marshall, Lasenby & Harris 1995).

Proceeding outward, we find the $2' - 3'$ shell of SgrA East (Eckers et al. 1983), which is characterized by a non–thermal radio emission with spectral index $\alpha = -0.64$. It is centered about $50''$ offset of SgrA* and is probably located behind SgrA West (Davies et al. 1976, Pedlar et al. 1989). Its synchrotron radio emission and its shell morphology were explained in terms of a supernova remnant. Mezger et al. (1989) discovered a dust ring compressed by the SgrA East shell, possibly indicating that this shell originated from an extremely energetic explosion (4×10^{52} ergs), maybe associated with SgrA*, occurring inside a dense molecular environment (10^4 cm^{-3}). Other alternative explanations are the simultaneous explosion of about 40 supernovae, or a single SN explosion inside a medium with a much lower density. In this case the dust shell could be due to the stellar wind from the normal supernova progenitor (Mezger et al. 1989). Another possibility is the tidal disruption of a star by the central supermassive black hole (Khokhlov & Melia 1996).

A triangular shaped non–thermal halo ($\sim$20 pc in diameter) surrounds in projection the SgrA East shell (Yusef-Zadeh & Morris 1987), but it is probably not physically related with it (see Pedlar et al. 1989 for a detailed discussion). Its origin is unknown. It could be centered at the SgrA* position and related with the high energy activity at the GC (Yusef-Zadeh et al. 1997, Melia et al. 1998). The total energy in relativistic particles estimated from radio observations is about 5×10^{50} ergs s^{-1}. This value, together with its non–thermal radio spectrum and its size, suggest the possibility that it is an evolved supernova remnant (Pedlar et al. 1989).

3. Observations and data analysis

Our results were obtained with the Medium Energy Concentrator Spectrometer (MECS, Boella et al. 1997) that provides images in the $\sim$ 1.3–10 keV energy range over a nearly circular field of view with $\sim 28'$ radius. The MECS has a good angular resolution (50% power radius of $\sim 75''$ at 6 keV, on-axis) and a moderate energy resolution (FWHM $\sim 8.5\sqrt{6/\mathrm{E_{keV}}}$%). In order to exploit the best spatial and spectral resolution of the detector, and to avoid the artifacts due to the absorbing strongbacks of the MECS entrance window, we only considered the inner region of the field of view (radius $\sim 8'$).

For the spectral analysis we have used the MECS effective area values appropriate for extended sources. These were properly derived by convolving a flat surface brightness distribution with the energy and position dependent vignetting and Point Spread Function (PSF).

All the spectra have been corrected for the the instrumental background by subtracting a spectrum obtained from MECS observations of the dark Earth. This procedure does not account for the subtraction of the cosmic X–ray background (CXB). Indeed, the subtraction of the MECS standard background obtained from high galactic latitude pointings would overestimate the CXB contribution, which is highly absorbed in the GC region. The CXB contribution has been included as a known additive component in the spectral fits with an absorbing column density of 8×10^{22} cm^{-2} and spectral parameters fixed at the values determined with the MECS (photon index = 1.44, F(1 keV)=12.9 phot cm^{-2} s^{-1} sr^{-1} keV^{-1}; S. Molendi, private communication).

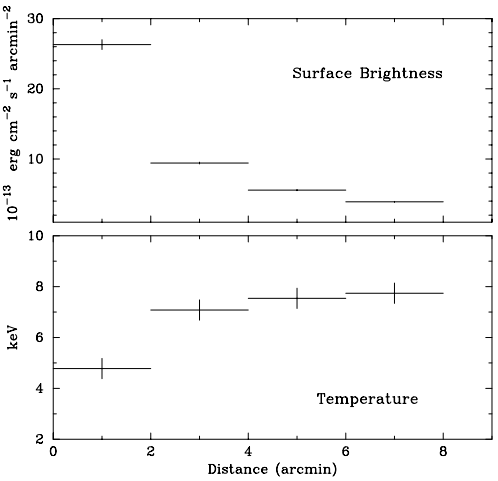

Fig. 2. Surface brightness and temperature in concentric regions around the GC.

4. X–rays from the Sgr A Complex

The location of SgrA* was imaged on August 24–26, 1997 for a net exposure time of 99.5 ks. In order to study the surface brightness and temperature profile of the diffuse emission, we extracted the MECS counts from four annular regions with different inner and outer radii ($0'-2'$,$2'-4'$,$4'-6'$,$6'-8'$) centered on SgrA*. All these spectra contain several emission lines, with the K-lines from iron (E~ 6.7 keV) and sulfur (E~ 2.4 keV) particularly bright. We fitted them with a single temperature plasma model (MEKAL in XSPEC v.10.00), deriving the surface brigthness and temperature profiles shown in Fig. 2. A radial spectral variation is evident: while the $\sim$ 7–8 keV temperature in the three external regions is almost constant, the emission from the inner $2'$ is significantly softer. This is probably due to the presence, in addition to the diffuse emission, of further contributions from the bright point sources present near the GC (Maeda et al. 1996, Predehl & Trümper 1994, Sidoli et al. 1999b).

The fit with a single temperature thermal model does not account for all the emission lines at low energies (in particular the intense emission from sulfur at E$\sim$2.4 keV), nor for an excess around 6.4 keV, due to the presence of emission of fluorescent origin. A gaussian line added at 6.4 keV accounts for these residuals. While this line is present in all the spectra extracted from $2'$ to $8'$, it seems to be absent within $2'$ (EW$\leq$12 eV). This is consistent with the 6.4 keV map produced with ASCA (Maeda & Koyama 1996) where a strong peak is visible in the region of the Radio Arc, NE to the GC. Indeed the EW of this line increases towards the outer regions ($EW_{2'-4'} = 80$–100 eV,$EW_{4'-6'} =$

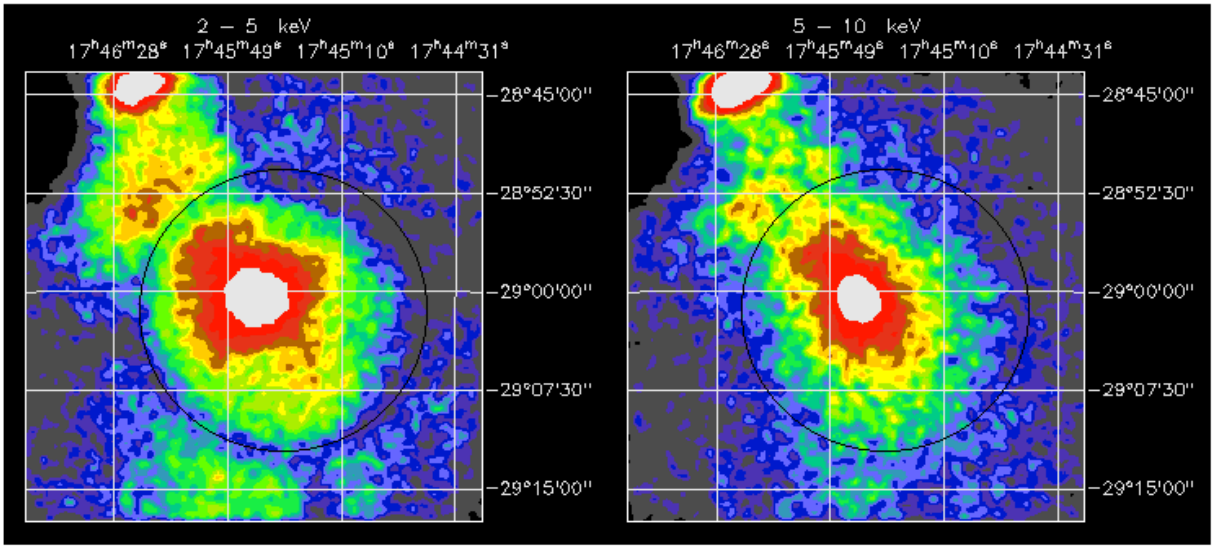

Fig. 3. 2–5 keV (left) and 5–10 keV (right) emission from the SgrA Complex. Both images have been smoothed with a gaussian with FWHM=1 arcmin. The strong source in the NE corner is 1E1743.1–2843 (Cremonesi et al. 1999). The low surface brightness in correspondence of the circle is an instrumental effect due to the absorption in the detector window support structure.

120–130 eV, $EW_{6'-8'} = 140$–150 eV). The MECS spectra extracted from two semi–annular regions at NE and SW of the GC, confirm this interpretation: the EWs of the 6.4 keV line are $\sim 100 \pm 30$ eV (NE sector; errors are at 90% confidence level) and $\sim 40 \pm 20$ eV (SW sector).

Since the temperature profile does not show evidence of strong spectral variations in the region from $2'$ to $8'$, we analysed the overall spectrum by extracting all the counts from this larger circular corona. We started by fitting a thermal bremsstrahlung plus three gaussian lines at ∼1.8, 2.4 and 6.7 keV (Si, S and Fe respectively). Their estimated equivalent widths are about 120, 190 and 1000 eV. The best fit value for the bremsstrahlung temperature is ∼13 keV. This temperature is too high to be consistent with the presence of the low energy emission lines (Kaneda et al. 1997, Fig. 2b). A possible explanation is a multi-temperature plasma. Thus we fitted the spectrum with two thermal emission plasma models (two "MEKAL" in XSPEC). Our best fit parameters (χ^2=1.29, 368 d.o.f) are $N_H = 7.93^{+0.09}_{-0.36} \times 10^{22}$ cm^{-2}, $T_1 = 0.57^{+0.02}_{-0.05}$ keV and $T_2 = 8.69^{+0.26}_{-0.41}$ keV. A gaussian added at 6.4 keV gives an EW∼120 eV. The total unabsorbed flux (2–10 keV) is $1.71^{+0.05}_{-0.08} \times 10^{-10}$ ergs cm^{-2} s^{-1}, about one third of which is contributed by the soft component.

To study the spatial distribution of the diffuse emission, we extracted images in different energy bands (Fig. 3). The images corresponding to the 2–5 keV and 7–10 keV ranges show significantly different distributions of the diffuse emission.

Both the soft and hard emissions are peaked at the GC position, but they have different spatial extents. In particular, the softer emission has a nearly triangular shape, with a rather sharp decrease in the south-western side, which is absent in the hard X–ray map. To study the spatial distribution of the iron line we have also extracted an image in the 5.5–7.5 keV band and subtracted from this map the continuum emission interpolated from the contiguous energies. The resulting iron line image shows a spatial distribution elongated along the galactic plane, very similar to that of the hard X–ray map.

5. Discussion

Our observation of the SgrA complex confirms the presence of a hot plasma with multiple temperatures and/or in non-equilibrium ionization, as already found with the ASCA instruments (Koyama et al. 1996). The increase in the 6.4 keV line equivalent width that we find in the North-East sector, is in agreement with the more detailed maps of this line obtained with ASCA that show a correlation with the molecular clouds. The limited spectral resolution of the MECS, compared with that of the ASCA solid state detectors, does not allow to study in more detail the energy profile and spatial distribution of the individual lines. On the other hand, the regular point spread function provided by the BeppoSAX mirrors has allowed us to produce unbiased maps in wide energy bands that demonstrate a clear difference in the spatial distribution of the softer and harder X–ray emission. Since also our spectral data could be well described by the sum of two thermal models with kT∼0.6 and 8 keV, it is tempting to give an interpretation in terms of two plasma components at different temperatures and with different spatial distributions (although in reality the situation is certainly much more complex, with, e.g., a distribution of temperatures). In this interpretation, it is remarkable that the lower temperature plasma is well correlated with the SgrA East triangular radio halo (Fig. 4).

The presence of unresolved point sources could affect the apparent distribution of the diffuse emission. We note however that previous observations, e.g. with Einstein and ROSAT (Watson et al. 1981, Predehl & Trümper 1994) do not show the presence of strong sources distributed in such a way to reproduce the triangular shape visible in our low energy map. In particular, the

straight contours of the soft emission corresponding to the SW side of the triangular radio halo seem hardly explainable by a distribution of sources. Although we cannot exclude that the apparent shape of the softer X–rays is due to an absorption effect, we favour the interpretation of the lower temperature plasma as a component physically related to the halo of SgrA East. In the following we will adopt this working hypothesis and assume a distance of 8.5 kpc.

We derive for the soft component an emission measure EM=(1.2±0.4) $\times 10^{14}$ cm^{-5}, which assuming emission from a spherical region with radius 10 pc and an electron filling factor f, corresponds to n$_e$ $\sim$ (3 $\times f^{-1/2}$) cm^{-3} and to a total mass $M_g \sim 250\ M_\odot f^{1/2}$.

The average thermal pressure in the SgrA East halo, $P \sim 3 \times 10^{-9}$ ergs cm^{-3}, is consistent with the pressure $P_{Sedov} = 0.106 \times (E_{SN}/R^3)$ ergs cm^{-3} derived for a SNR in a Sedov phase, where E_{SN} is the explosion energy of the SNR and R is the shell radius in cm. Indeed, if we assume $E_{SN} = 10^{51}$ ergs s^{-1} and R=10 pc, we find $P_{Sedov} \sim 4 \times 10^{-9}$ ergs cm^{-3}.

The X–ray luminosity (2–10 keV) of the soft component is $\sim 4.5 \times 10^{35}$ ergs s^{-1}. If we assume that this thermal emission is mostly produced by the SgrA East halo, its X–ray luminosity, pressure, density, temperature of the emitting gas (0.6 keV) and size (∼20 pc), match well with a supernova remnant origin in which thermal line emission is produced when the expanding supernova ejecta heats the ISM to X–ray temperatures.

Another test of the SNR hypothesis can be done by comparing the X–ray and radio surface brightnesses: indeed a strong correlation $\Sigma_R \propto \Sigma_X^{0.69\pm0.08}$ between the radio Σ_R (at 1 GHz) and the X–ray surface brightness Σ_X (0.15–4.5 keV) was found by Berkhuijsen (1986). From the radio spectrum reported by Pedlar et al. (1989) we derived $\Sigma_R \sim 5 \times 10^{-19}$ W m^{-2} Hz^{-1} sr^{-1}. The Σ_X measured from our X–ray data and converted to the 0.15–4.5 energy band is $\Sigma_X \sim 10^{34}$ ergs s^{-1} pc^{-2}. These values fall well inside the region defined by other typical SNRs.

In conclusion, all the physical quantities derived from the analysis of the MECS are consistent with a SNR origin for the SgrA East halo.

6. Conclusions

The analysis of the diffuse emission from the GC region reveals the presence of at least two distinct components: a soft one (T$_{mekal}$ ∼0.6 keV), spatially correlated with the SgrA East radio halo and a hard component (T$_{mekal}$ ∼8–9 keV). While the hard component is elongated along the Galactic Plane and does not spatially correlate with physical structures observed at other wavelengths, the spatial distribution of the soft component is remarkably well correlated with the triangular radio halo of SgrA East. The parameters derived for the softer component match extremely well with the idea that this thermal X–ray emission is due to a SNR origin for the SgrA East halo.

Acknowledgements. We thank L. Chiappetti, G. Matt, S. Molendi and A. Treves for useful discussions and help with the data analysis.

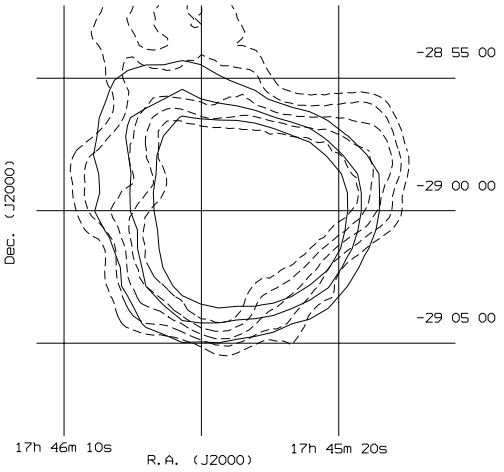

Fig. 4. Contour levels of the 2–5 keV emission overlayed on the 90 cm radio contours (dashed line, adapted from Anantharamaiah et al. 1991).

References

Anantharamaiah K.R., Pedlar A., Ekers R.D., Goss W.M. 1991, MNRAS 249, 262
Balick B., Brown R.L. 1974, ApJ 194, 265
Berkhuijsen E.M., 1986, A&A 166, 257
Boella G. et al., 1997, A&AS 122, 327
Cremonesi D.I., Mereghetti S., Sidoli L., Israel G.L., 1999, A&A 345, 826
Davies R.D., Walsh D., Booth R.S. 1976, MNRAS 177, 319
Eckers R.D, van Gorkom J.H, Schwarz U.J., Goss W.M. 1983, A&A 122, 143
Ghez A.M., Klein B.L., Morris M., Becklin E.E. 1998, ApJ 509, 678
Kaneda H. et al. 1997, ApJ 491, 638
Kawai N. et al. 1988, ApJ 330, 130
Khokhlov A., Melia F. 1996, ApJ 457, L61
Koyama K. et al. 1989, Nature 339, 603
Koyama K. et al. 1996, PASJ 48, 249
Krichbaum T.P. et al. 1998, A&A 335, L106
Lo K.Y., Shen Z., Zhao J., Ho P.T.P 1998, ApJ 508, 61
Marshall J., Lasenby A.N., Harris A.I. 1995, MNRAS 277, 594
Maeda Y. et al. 1996, PASJ 48, 417
Maeda Y., Koyama K. 1996, ASP Conf. Ser. 102, p. 423
Melia F. Fatuzzo M., Yusef-Zadeh F., Markoff S. 1998, ApJ 508, 65
Mezger P.G. et al. 1989, A&A 209, 337
Mezger P.G., Duschl W.J., Zylka R. 1996, A&AR 7, 289
Morris M., Serabyn E. 1996, ARAA 34, 645
Pedlar A. et al. 1989, ApJ 342, 769
Predehl P., Trümper J. 1994, A&A 290, L29
Reid M.J. et al. 1999, AAS 194, 5014
Sidoli L. et al., 1998, Proc. XTE/SAX Symp. "The Active X–ray Sky", Rome 1998, p.88
Sidoli L. et al., 1999a, Proc. Third INTEGRAL Workshop, "The Extreme Universe", Taormina 1998, in press
Sidoli L., Mereghetti S., Israel G.L., et al. 1999b, ApJ in press
Skinner G.K. et al. 1987, Nature 330, 544
Yusef-Zadeh F., Morris M. 1987, ApJ 320, 545
Yusef-Zadeh F., Purcell W., Gotthelf E. 1997, Proc. 4^{th} Compton Symp., p.1027
Yusef-Zadeh F. et al. 1999, astro-ph/9904381
Yusef-Zadeh F., Choate D., Cotton W. 1999, ApJ 518, 33
Watson M.G., Willingale R., Grindlay J.E., Hertz P. 1981, ApJ 250, 142
Zane S., Turolla R., Treves A. 1996, ApJ 471, 248